EQUILIBRIUM AND BALLOONING STABILITY OF RESISTIVE TOKAMAK PLASMAS NEAR THE SEPARATRIX

H.P. Zehrfeld

Max-Planck-Institut für Plasmaphysik, EURATOM Association,
D-85748 Garching

Equilibrium and ballooning stability of resistive plasmas for given density, temperature and z-effective profiles is considered. Pressure and resistivity profiles are determined by an equation of state and a neoclassical description of parallel resistivity, respectively. The poloidal current distribution is obtained by solving the equilibrium problem taking into account Ohm's law. Obtaining in this way a diffusing plasma, the equilibria are characterized by the appearence of electric fields and of flow. These as well as ballooning stability are discussed in connection with profiles showing a pedestal-like structure near the separatrix.

1. Introduction

In previous work [1] the ballooning stability of tokamak divertor equilibria with steep pressure gradients in the immediate neighbourhood of the separatrix was studied. It was found that the ideal-ballooning stability boundaries as well as the growth rates of the corresponding resistive modes depend, besides on the chosen pressure profiles, in a sensible way on the poloidal current distribution. In the investigation [2] on ideal ballooning modes using a local equilibrium model a distribution was chosen which corresponds to high plasma resistivity near the separatrix. Here we extend this approach to global tokamak equilibria with non-zero edge current densities.

More generally, in discussing the physical reasons for a particular form of the poloidal current profile it is observed that potential contributions such as bootstrap [3] or quasi-stationary currents coming from an Ohmic transformer [4]. appear in the form of the flux-surface average $\langle\, \mathbf{j}\cdot\mathbf{B}\,\rangle$, so that a corresponding reformulation and solution of the equilibrium problem becomes necessary.

2. Theory

The equilibrium partial differential equation with the current density written in its standard form is

$$\mathrm{R}^2 \mathrm{div}\frac{\nabla\Psi}{\mathrm{R}^2} = -2\pi\mu_0 \mathrm{R} \mathrm{j}_\mathrm{T}, \qquad \mathrm{j}_\mathrm{T} \equiv \frac{\mu_0}{4\pi\mathrm{R}}\frac{\mathrm{dJ}^2}{\mathrm{d}\Psi} + 2\pi\mathrm{R}\frac{\mathrm{dp}}{\mathrm{d}\Psi} \tag{1}$$

We consider separatrix-defined solutions of this equation for given plasma current $\mathrm{I_p}$ controlled by a vacuum magnetic field part of Ψ so that the magnetic axis is at a fixed position. We use the notations $\mathrm{I} = \mathrm{I}(\mathrm{V})$ for the toroidal current, where V is the volume of a magnetic surface, and re-write the current density by replacing the term containing the $\mathrm{dJ}^2/\mathrm{d}\Psi$ by the flux-surface average of the parallel current $\mathbf{j}\cdot\mathbf{B}/(\mu_0\mathrm{J})$

$$\mathrm{j}_\mathrm{T} = 2\pi\mathrm{R}\left\{\mathrm{N}(\mathrm{R})\mathrm{F}_\mathrm{B}\frac{\langle\, \mathbf{j}\cdot\mathbf{B}\,\rangle}{\mu_0\mathrm{J}} + (1-\mathrm{N}(\mathrm{R})\mathrm{F}_\mathrm{B})\frac{\mathrm{dp}}{\mathrm{d}\Psi}\right\} \tag{2}$$

where the dimensionless quantities $\mathrm{F_B}$ and N are given by

$$\mathrm{F}_\mathrm{B}(\mathrm{I},\mathrm{J}) = \frac{\langle\, \mathrm{B}_\mathrm{T}^2\,\rangle}{\langle\, \mathrm{B}^2\,\rangle} = \left\{1 + \mathrm{L}_\mathrm{R}\frac{\mathrm{I}^2}{\mathrm{J}^2}\right\}^{-1}, \qquad \mathrm{N}(\mathrm{R}) = \frac{\langle\, 1/\mathrm{R}^2\,\rangle^{-1}}{\mathrm{R}^2} \tag{3}$$

and $\mathrm{L_R}$ is a geometric inductance coefficient

$$\mathrm{L_R} \equiv \frac{16\pi^4}{\langle\, 1/\mathrm{R}^2\,\rangle\langle\, |\nabla \mathrm{V}|^2/\mathrm{R}^2\,\rangle} \tag{4}$$

I and J – for given functions $\langle\, \mathbf{j}\cdot\mathbf{B}\,\rangle/(\mu_0 \mathrm{J})$ and $\mathrm{dp}/\mathrm{d}\Psi$ – must be determined solving the two-point nonlinear boundary value problem

$$\frac{\mathrm{dI}}{\mathrm{dV}} = \mathrm{F_B}(\mathrm{I},\mathrm{J})\frac{\mathrm{C_s}\langle\, \mathbf{j}\cdot\mathbf{B}\,\rangle}{\mu_0 \mathrm{J}} + (1-\mathrm{F_B}(\mathrm{I},\mathrm{J}))\frac{\mathrm{dp}}{\mathrm{d}\Psi} \tag{5}$$

$$\frac{1}{2}\frac{\mathrm{dJ}^2}{\mathrm{dV}} = \mathrm{L_R I F_B}(\mathrm{I},\mathrm{J})\left\{-\frac{\mathrm{C_s}\langle\, \mathbf{j}\cdot\mathbf{B}\,\rangle}{\mu_0 \mathrm{J}} + \frac{\mathrm{dp}}{\mathrm{d}\Psi}\right\} \tag{6}$$

together with (1). Equation (5) describes equilibrium on average. (6) is the differential relation connecting $\langle\, \mathbf{j}\cdot\mathbf{B}\,\rangle$ and $\mathrm{dJ}^2/\mathrm{d}\Psi$. Both in (5) and (6) a scaling factor $\mathrm{C_s}$ is necessary which must be determined so that the conditions $\mathrm{I}=0$ on axis and $\mathrm{I}=\mathrm{I_p}$ and $\mathrm{J}=\mathrm{J_B}$ at the separatrix are satisfied. This is achieved by adding a third equation $\mathrm{dC_s}/\mathrm{dV}=0$ leading to three equations for I, J and $\mathrm{C_s}$ with the correct number of boundary conditions. Note the similarity between (2) and (5). $\langle\, \mathbf{j}\cdot\mathbf{B}\,\rangle/(\mu_0 \mathrm{J})$ (which on axis is $\mathrm{jT}/2\pi\mathrm{R}$) and $\mathrm{dp}/\mathrm{d}\Psi$ have the common dimension $[\mathrm{A}/\mathrm{m}^3]$.

3. Calculations

Fig. 1 shows profiles $\langle\, \mathbf{j}\cdot\mathbf{B}\,\rangle$ which apply for temperature, density and z-effective distributions of an ASDEX Upgrade equilibrium resulting in the pressure and pressure gradient distributions of Fig. 2(a). Except the axis and boundary regions, where $\langle\, \mathbf{j}\cdot\mathbf{B}\,\rangle_{\mathrm{BS}}$ vanishes, they are similar in form.

Here we present calculations for equilibrium and ballooning stability which have been done using the $\langle\, \mathbf{j}\cdot\mathbf{B}\,\rangle/(\mu_0 \mathrm{J})$-term valid for a resistive plasma which is obtained from the parallel component of Ohm's law and where $\mathrm{C_s}$ can be identified with the loop voltage U:

$$\frac{\langle\, \mathbf{j}\cdot\mathbf{B}\,\rangle_{\mathrm{RP}}}{\mu_0 \mathrm{J}} = \frac{\mathrm{U}\langle\, 1/\mathrm{R}^2\,\rangle}{4\pi^2\eta_{\|}} \tag{7}$$

$\langle\, \mathbf{j}\cdot\mathbf{B}\,\rangle_{\mathrm{RP}}$ shows a pedestal-like structure near the separatrix inherited from the $\mathrm{T_e}$–profile and has a close relationship to the rotational transform $\iota = 1/\mathrm{q}$ as

$$\frac{\mathrm{d}(\iota/\mathrm{L_R})}{\mathrm{dV}} = \frac{\mathrm{U}\langle\, 1/\mathrm{R}^2\,\rangle}{4\pi^2\eta_{\|}\mathrm{J}} \tag{8}$$

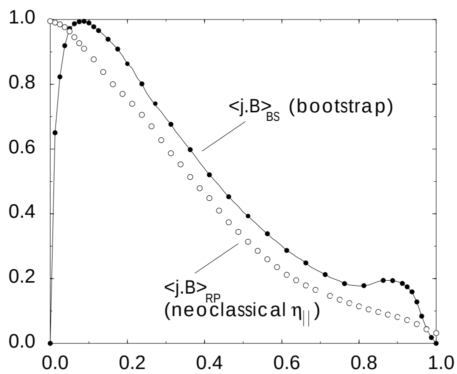

Fig. 1: $\langle\, \mathbf{j}\cdot\mathbf{B}\,\rangle$ normalized by its maximum vs. normalized flux.

Even in cases where due to the persistence of inductive effects (7) might be not a good description of the plasma core, (8) can serve as a convenient aid for q-profile shaping by suitably modifiying $\eta_{\|}$. In this way always a uniform and continuous profiling from axis to boundary for the purpose of equilibrium calculations is possible.

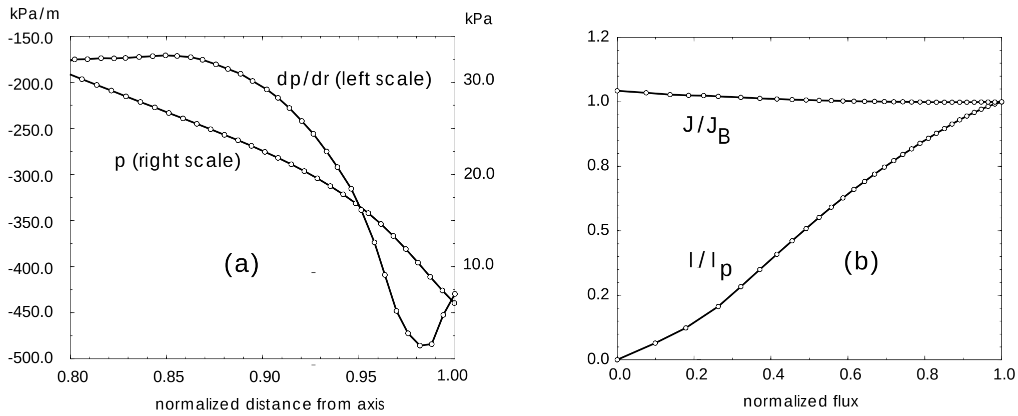

Fig. 2: (a) Edge pressure and pressure gradient distributions along a straight line leading from the magnetic axis to the outer side of the separatrix. (b) The currents I and J as obtained as solutions of equations (5,6).

Solving equation (6) makes the electric potential φ_{s} in the parallel component of Ohm's law single-valued. This can be seen by flux-surface averaging

$$\mathbf{B}\cdot\nabla\varphi_{\mathrm{s}} = -\mu_0 \mathrm{J}\left\{\eta_{\|}\left(1-\frac{\mathrm{B}^2}{\langle\,\mathrm{B}^2\,\rangle}\right)\frac{\mathrm{dp}}{\mathrm{d}\Psi} + \frac{\mathrm{U}}{\mu_0^2\mathrm{J}^2}\left(\mathrm{B}_{\mathrm{p}}^2 - \langle\,\mathrm{B}_{\mathrm{p}}^2\,\rangle\frac{\mathrm{B}^2}{\langle\,\mathrm{B}^2\,\rangle}\right)\right\} \tag{9}$$

Note that at plasma boundary $\partial\varphi_{\mathrm{s}}/\partial\mathrm{s}$ (s being the arc length along the separatrix) has a pole at the x-point, whereas φ_{s} is smooth and finite there. Due to the term scaling as $\partial\varphi_{\mathrm{s}}/\partial\mathrm{s} \propto \eta_{\|}(\mathrm{B_T}/\mathrm{B_p^2})(\mathrm{dp}/\mathrm{dr})$ steep edge gradients of the pressure cause sheared electric fields near the separatrix (Fig. 3(c)). Moreover, the presence of the electric potential φ_{s} implies flow perpendicular to $\mathbf{B}$

$$\mathbf{v}_\perp = \frac{1}{\mathrm{B}^2}\left\{\mathbf{B}\times\nabla\varphi_{\mathrm{s}} + \left(\frac{\mathrm{U}}{4\pi^2\mathrm{R}^2} + \eta_\perp\frac{\mathrm{dp}}{\mathrm{d}\Psi}\right)\nabla\Psi\right\} \tag{10}$$

and, due to mass conservation, also parallel to $\mathbf{B}$:

$$\mathbf{B}\cdot\nabla(\mathrm{v}_\|/\mathrm{B}) = -\frac{1}{\rho}\mathrm{div}\left\{\frac{\rho}{\mathrm{B}^2}\left\{\nabla\varphi_{\mathrm{s}}\times\mathbf{B} - \left(\frac{\mathrm{U}}{4\pi^2\mathrm{R}^2} + \eta_\perp\frac{\mathrm{dp}}{\mathrm{d}\Psi}\right)\nabla\Psi\right\}\right\} - \frac{\mathrm{Q_M}}{\rho} \tag{11}$$

The most general flow caused and allowed by the equations is then

$$\mathbf{v} = \mathbf{v}_{\mathrm{s}} + \mathrm{S_s}(\Psi)\mathbf{B} + \Omega_{\mathrm{s}}(\Psi)\mathrm{R}^2\nabla\varphi \tag{12}$$

$\mathbf{v}_{\mathrm{s}}$ is the special solution obtained from above with $\varphi_{\mathrm{s}} = \mathrm{v}_\| = 0$ on some reference line leading from the magnetic axis to the plasma boundary and $\mathrm{S_s}$ and Ω_{s} are free functions.

4. Results on Ballooning Stability

Stability against ideal ballooning modes is determined by the solution of the corresponding Sturm-Liouville problem:

$$\frac{\mathrm{d}}{\mathrm{d}\theta}\left(\mathrm{P}\frac{\mathrm{dU}}{\mathrm{d}\theta}\right) + \mathrm{QU} = 0 \tag{13}$$

$$\mathrm{P} = \frac{\mathbf{B}\cdot\nabla\theta(1+\mathrm{S}^2)}{|\nabla\Psi|^2}, \quad \mathrm{Q} = -\frac{2\mu_0(\kappa_{\mathrm{n}} - \mathrm{S}\kappa_{\mathrm{g}})}{\mathbf{B}\cdot\nabla\theta|\nabla\Psi|}\mathrm{P_s}\frac{\mathrm{dp}}{\mathrm{d}\Psi}, \quad \mathrm{S} = \frac{|\nabla\Psi|^2}{\mathrm{B}}\left[\frac{\mathrm{dq}}{\mathrm{d}\Psi}\frac{\theta}{2\pi} - \mathrm{P_sT_p}\right]_{\theta_{\mathrm{LP}}}^{\theta} \tag{14}$$

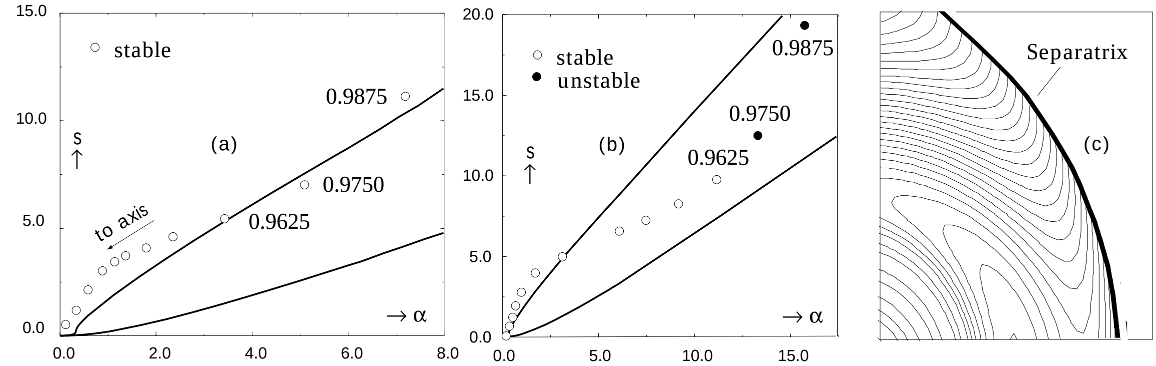

Fig. 3: Equilibrium (α, s)-values on flux surfaces tested for ballooning stability. (a) for moderate, (b) for steep plasma pressure edge pedestals. (c): Contours of constant electric potential φ_s

The evaluation of S refers to the point under consideration (θ) and the localization point poloidal angle $\theta = \theta_{\mathrm{LP}}$. $\mathrm{T_p}$ is a periodic function describing diamagnetic effects and effects of elongation and triangularity. $\mathrm{P_s}$ in (14) is an arbitrary scaling factor for showing up expected pressure gradient and second stability effects without calculating new equilibria. The high-n stability of the calculated equilibria was tested with the Garching ballooning code GARBO. The mode localization points were positioned on the straight line of length $\mathrm{r_s}$ leading from the magnetic axis to the outer side of the separatrix. The results are presented in Figs. 3 (a) and (b) as circles labeled by the corresponding normalized flux value $\mathrm{X} \in (0, 1)$. For orientation also the stability boundaries valid for the simple $\alpha - \mathrm{s}$ model are drawn, where the following definitions have been used: $\alpha = -2\mu_0 \mathrm{q}^2 \mathrm{R}(\mathrm{dp}/\mathrm{dr})/\mathrm{B_T^2}$ and $\mathrm{s} = (\mathrm{r}/\mathrm{q})(\mathrm{dq}/\mathrm{dr})$. Here R and $\mathrm{B_T}$ were inserted with their values at the axis and $\mathrm{r} = \mathrm{r_s}\sqrt{\mathrm{X}}$. Fig. 3(a) shows results for the pressure gradients of Fig. 2(a). As $\mathrm{dp}/\mathrm{d}\Psi \simeq -(\mathrm{dp}/\mathrm{dr})/(2\pi \mathrm{R}\mathrm{B_p})$ and spatial measurements have been used, $\mathrm{dp}/\mathrm{d}\Psi$ was updated for each iteration cycle during the equilibrium calculation. Interpreting the measured $\mathrm{T_e}$ and $\mathrm{T_i}$ profiles more aggressively towards the stability limit, the picture of Fig. 3(b) with edge pressure gradients greater by a factor of about 1.8 was obtained. The two surfaces marked as unstable cross the radial line described above at distances of 0.37cm and 0.74cm from the outer side of the separatrix. The expected pressure gradient scales for entering the first unstable regime is about 0.9, that for transition into second stability approximately 1.2.

References

[1] H.P. Zehrfeld and J. Geiger: "Growth Rates of Resistive Ballooning Modes in ASDEX Upgrade and W7-AS", in *24th EPS Conference on Controlled Fusion, Contributed Papers*, page 1561, Berchtesgaden, Germany, 1997.

[2] C. Bishop: "Stability of Localized MHD Modes in Divertor Tokamaks – a Picture of the H-Mode", Nucl. Fusion **26**, 1063 (1986).

[3] C. Kessel: "Bootstrap Current in a Tokamak", Nucl. Fusion **34**, 1221 (1994).

[4] H.P. Zehrfeld and F. Casci: "Calculation of Axially Symmetric Resistive Steady-State Plasma Equilibria in terms of Pressure Distributions", Computer Physics Communications **31**, 155–165 (1984).